

# Synthesis and Reconstruction of Fingerprints using Generative Adversarial Networks

Rafael Bouzaglo and Yosi Keller

**Abstract**—Deep learning-based models have been shown to improve the accuracy of fingerprint recognition. While these algorithms show exceptional performance, they require large-scale fingerprint datasets for training and evaluation. In this work, we propose a novel fingerprint synthesis and reconstruction framework based on the StyleGan2 architecture, to address the privacy issues related to the acquisition of such large-scale datasets. We also derive a computational approach to modify the attributes of the generated fingerprint while preserving their identity. This allows for the simultaneous synthesis of multiple different fingerprint images per finger. In particular, we introduce the SynFing synthetic fingerprints dataset consisting of 100K image pairs, each pair corresponding to the same identity. The proposed framework was experimentally shown to outperform contemporary state-of-the-art approaches for both fingerprint synthesis and reconstruction. It significantly improved the realism of the generated fingerprints, both visually and in terms of their ability to spoof fingerprint-based verification systems. The code and fingerprints dataset are publicly available: <https://github.com/rafaelbou/fingerprint-generator/>.

**Index Terms**—Deep Learning, Fingerprint Synthesis, Fingerprint Reconstruction, Generative Adversarial Networks

## I. INTRODUCTION

Human fingerprints are one of the most common biometric attributes used for authentication and identification, from border control identification to payment authorization to the daily use of unlocking electronic devices such as cellphones [1], [2]. Current state-of-the-art fingerprint recognition systems are mostly based on deep learning models [3], [4]. While these systems show exceptional performance, they require expensive large-scale fingerprint datasets for training and evaluation. Furthermore, collecting and sharing large-scale biometric datasets comes with inherent risks and privacy concerns. For example, the National Institute of Standards and Technology (NIST) recently discontinued several publicly available datasets from its catalog due to privacy issues [5].

To alleviate both cost and privacy issues, several approaches have been proposed to create synthetic fingerprint datasets. Their goal is to produce large datasets of synthetic fingerprints that can be used instead of datasets of real fingerprints. The two core tasks associated with the generation of synthetic fingerprints are the synthesis [7], [8], [9], [10] and reconstruction [11], [12], [13], [14] that are shown in Fig.

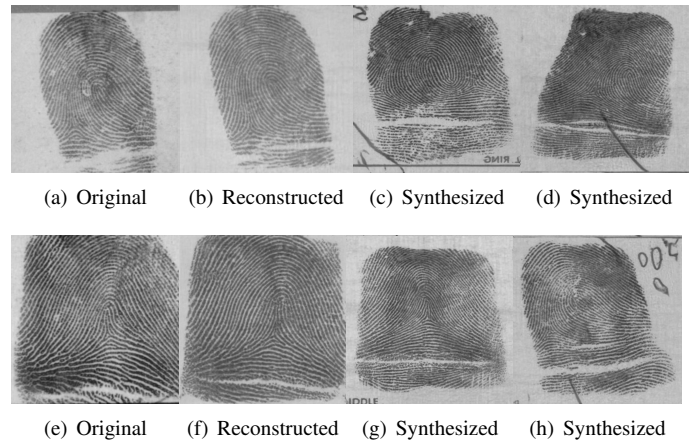


Fig. 1. The proposed reconstruction and synthesis of fingerprints. (b) and (f) are the reconstructions of (a) and (e), respectively, based on their minutiae points. (a) and (e) were taken from the NIST SD4 dataset [6]. (c), (d), (g) and (h) are examples of randomly synthesized fingerprints.

1. The goal of fingerprint synthesis is to generate synthetic fingerprints that are as realistic as possible, while the goal of fingerprint reconstruction is to generate synthetic fingerprints resembling the source fingerprints as close as possible. In fingerprint reconstruction, a set of features extracted from a given fingerprint, typically minutiae [11], are provided, while in fingerprint synthesis no input is given.

The common approach to fingerprint synthesis and fingerprint reconstruction is model-based, where multiple computational models are used to estimate the different attributes of the generated fingerprint: pattern area, orientation image, and ridge pattern. Rendering is then applied to improve the realism of the reconstructed fingerprint [7], [8], [11], [15]. The fingerprints generated using these approaches lack the inherent constraints between the orientation field, ridge valley structure, and minutiae patterns, leading to unrealistic fingerprint images, easily distinguishable from real fingerprints [16]. More recently, learning-based approaches, based mainly on the Generative Adversarial Networks (GAN) architecture [17], have been applied to fingerprint synthesis [9], [10], [18], [19]. Contrary to model-based approaches, GANs learn to generate fingerprint images adhering to the probability distribution of *fingerprint images*, rather than the attributes of the fingerprints, in the training set. Although such approaches improve the realism of the generated fingerprint images, the synthesized fingerprints do not adhere to the fundamental attributes of real

R. Bouzaglo & Y. Keller are with the Faculty of Engineering, Bar-Ilan University, E-mail: yosi.keller@gmail.com

Manuscript received April 19, 2005; revised August 26, 2015.

fingerprints as the synthesis is based on random inputs. The distributions of the minutiae of the fingerprints are not random, and different types of fingerprints have different distributions of the minutiae. Therefore, the distributions of minutiae of synthetically generated fingerprints do not conform to such distributions. Another limitation of both the synthesis and the fingerprint reconstruction approaches is their inability to control the visual attributes of a fingerprint, such as the presence or absence of fingerprint artifacts, background noise, and fingerprint shape. By altering fingerprint attributes, a user can generate large datasets of fingerprints to address image-level and minutiae-level fingerprint matching, artifact removal, minutiae extraction, and fingerprint enhancement.

In this work, we propose a joint framework for fingerprint synthesis and reconstruction, allowing one to create a wide range of synthetic fingerprint datasets for a gamut of applications. The core of our approach is a fingerprint generator based on the Stylegan2 architecture [20], which is trained on a large dataset of fingerprints. The generator produces a realistic fingerprint image, based on a latent vector input. A random fingerprint can be synthesized by feeding the generator with a random vector. For fingerprint reconstruction, we propose an encoder network to encode minutiae attributes as latent vectors, such that the fingerprint generator can reconstruct the source fingerprint. To preserve the identity of the synthesized and reconstructed fingerprints, we derive a novel fingerprints-oriented perceptual loss based on the FingerNet CNN [21]. We also present a novel approach for modifying particular visual attributes of the fingerprint, such as blobs and dry skin artifacts, while preserving its identity. By applying this framework, we synthesize and share the SynFing dataset, consisting of 100K pairs of fingerprint image, each pair having the same identity but different visual attributes. This dataset can be used to train, validate, and spoof COTS fingerprints verification systems.

In particular, we propose the following contributions:

- We present a novel joint framework for fingerprints synthesis and reconstruction based on Generative Adversarial Networks and the encoding of fingerprint attributes.
- The proposed encoder and generator are trained using a novel minutiae encoding and fingerprint-oriented perceptual loss based on FingerNet CNN [21], which has been shown to improve the accuracy of reconstruction.
- The framework introduces a novel computational approach to modify and manipulate the visual attributes of the generated fingerprint image. This allows to generate multiple fingerprint images for each fingerprint identity.
- We introduce and share the large-scale SynFing dataset of synthetic fingerprints that can be applied to fingerprint matching, artifacts removal, and fingerprint spoof detection.
- The proposed framework was experimentally shown to

outperform contemporary approaches for fingerprint synthesis and fingerprint reconstruction.

## II. RELATED WORK

### A. Fingerprint Synthesis

Cappelli et al. [22] were the first to propose a model-based approach to fingerprint synthesis, using multiple generation steps, generating directional and density maps, ridge patterns, adding noise, and rendering. They use the fingerprint's type, size, and singular points as input. A Gabor-like space-variant filter and a modified Zero Pole model were applied to generate a near-binary fingerprint image. Then, task-specific noise is added to generate a realistic gray-scale representation of the fingerprint. Although these methods are relatively simple and do not require a large fingerprint database for model calibration, they generated unrealistic fingerprints. In particular, Gottschlich et al. [16] demonstrated their ability to differentiate between genuine and synthetic fingerprints by examining the distribution of the minutiae points.

Recent learning-based approaches for fingerprint synthesis utilized generative adversarial networks (GANs), where the generation is based on processing a noise vector through a generative model to generate a synthetic fingerprint image. The generative model is trained using a large fingerprint dataset. Minaee et al. [9] used the DCGAN [23] architecture with a total variation regularization term to impose connectivity within the generated images, while Mistry et al. [10] applied an Improved Wasserstein GAN (IWGAN) [24]. Recently, Bahmani et al. [19] introduced the Clarkson Fingerprint Generator based on the StyleGan [25] architecture.

### B. Fingerprint Reconstruction

Fingerprint reconstruction is the synthesis of fingerprints based on given attributes, such as minutiae templates. The reconstructed fingerprint aims to reproduce the minute locations and distribution in the original fingerprint. Contemporary reconstruction schemes follow two steps: first, reconstruct the orientation field based on minutiae, and then reconstruct the ridge pattern using the reconstructed orientation field. Cappelli et al. [11] proposed to reconstruct the grayscale image directly using the minutiae. The orientation field was reconstructed by a zero-pole model, followed by iterative Gabor filtering of the minutiae image initialized by the local minutiae pattern. Using a disk-shaped structuring element, Feng et al. [12] predicted the local orientation values, where the rigid pattern was reconstructed using the amplitude and frequency modulated model (AM-FM) [26]. Cao et al. [13] proposed a dictionary-based approach to fingerprint reconstruction, where a dictionary of orientation patches is used to reconstruct the orientation field from minutiae, while the continuous phase patch dictionary is used to reconstruct the ridge pattern. Similarly to fingerprint synthesis, recent fingerprint restoration models utilize the GANs generation approach. Kin et

al. [27] applied conditional GANs to minutiae images by formulating fingerprint reconstruction as an image-to-image translation, in which a fingerprint image is generated from an image containing minutiae information. Similarly, Moon et al. [14] use Pix2Pix [28] to improve the reconstruction accuracy. However, the matching accuracy of the reconstructed fingerprints was significantly inferior to that of the original fingerprint images. Moreover, none of these works made their reconstruction models publicly available, hindering the reproducibility and the fair comparison between models, as their results are reported for private datasets only [14], [27].

### III. FINGERPRINT SYNTHESIS AND RECONSTRUCTION

We propose a joint framework for fingerprint synthesis and reconstruction, whose overview is shown in Fig. 2. Our fingerprint generator, detailed in Section III-A, is based on the StyleGAN2 architecture [20] (G in Fig. 2), trained using the NIST SD14 fingerprint dataset to synthesize fingerprint images. To generate a new fingerprint image, we feed the generator G with a latent vector  $w$ . In the synthesis branch, a normal distribution generator is used to randomly generate  $w$ , which is input into the generator G to synthesize a realistic fingerprint image. In the reconstruction branch, detailed in Section III-B, we train a Minutiae-To-Vec encoder network E to encode the minutiae information extracted from a particular fingerprint into a latent vector  $w$ , used to reconstruct the original fingerprint. The proposed Fingerprint Attribute Editor A (Section III-D) is added before the input layer of the generator G, to allow the user to manipulate the latent code  $w$  to modify particular attributes of the generated fingerprint, while preserving its identity.

#### A. Fingerprint Generator

The proposed fingerprint generator is based on the StyleGAN2 architecture [20] that is given a latent vector  $z \in \mathbb{R}^{512} \sim P_z$ , where  $P_z$  is a multivariate Gaussian distribution. Unlike traditional generators, in which  $z$  is directly passed into the convolutional upscaling layers, the StyleGAN2 generator uses a multistage input block to map  $z$  to a style vector  $y$ . Thus, the latent vector  $z$  is mapped to an intermediate latent vector  $w$ , using an 8-layer MLP network  $f : z \rightarrow w$ , then learned affine transformations specialize  $w$  to multiple style vectors  $y$ . Each style vector is fed into a different convolution layer of the generator. The output of the generator is a grayscale image  $I \in \mathbb{R}^{h \times w}$ .

#### B. Fingerprint Reconstruction

Let  $x \in \mathbb{R}^{h \times w \times 3}$  be a fingerprint image and  $S_x = \{\theta_{ij}, T_{ij}\}$  is the set of minutiae extracted from  $x$  at the points  $\{i, j\}$ , where  $\theta_{ij}$  and  $T_{ij}$  are the direction and class of the minutia, respectively. The reconstruction model reconstructs the fingerprint image  $x$  given  $S_x$ . We cast the fingerprint reconstruction as image-to-image translation [29], [30] where the minutiae set is first converted to a minutiae map  $M_x \in \mathbb{R}^{h \times w \times 3}$  following

[27], [31], [32].  $M_x$  is encoded by a latent vector  $w \in \mathbb{R}^{512}$  using a Minutiae-To-Style CNN (Section III-C), that is fed to the pretrained generator G to reconstruct the input image  $x$ .

#### C. Minutiae-To-Vec Encoder

Given a minutia set  $S_x$  of the fingerprint image  $x \in \mathbb{R}^{h \times w \times 3}$ , its corresponding minutia map  $M_x \in \mathbb{R}^{h \times w \times 3}$  is given by

$$M_x^{i,j} = \begin{cases} |l(\theta_{ij}), 0, 0| & T_{ij} \text{ is a Bifurcation point} \\ 0, l(\theta_{ij}), 0 & T_{ij} \text{ is a Termination point} \\ 0, 0, l(\theta_{ij}) & T_{ij} \text{ is a Singular point} \\ 0, 0, 0 & \text{otherwise} \end{cases} \quad (1)$$

For each location  $(i, j) \in S_x$  we draw a line  $l(\theta_{ij})$  in orientation  $\theta_{ij}$  that is drawn at the point in the channel corresponding to the class of minutiae  $T_{ij}$  as in Eq. 1.  $M_x$  is convolved with a Gaussian kernel  $G(\sigma)$  to create a smoother minutiae map. Minutia maps are shown in Fig. 3. The encoder E encodes  $M_x$  as the latent vector  $w \in \mathbb{R}^{512}$ , used by the generator to generate a fingerprint with the same attributes as the original. These properties include the finger type, fingerprint shape, internal interactions between minutiae points, singular areas, and the locations, types and orientations of the minutiae points. We applied the ResNet50 CNN [33] as the encoder network E to compute  $w$ , by adding a fully-connected layer following its last convolutional layer.

#### D. Fingerprint Attributes Editor

The proposed fingerprint generation approach allows modifying the attributes of the generated fingerprints, while preserving their identity (minutiae, rigid pattern, and finger type). Such attributes are the appearance of artifacts, acquisition position, and appearance of noises in the background. Thus, a user can generate multiple *different* impressions of the same fingerprint, remove noise and artifacts, and apply image-level fingerprint matching.

For that, we follow the SeFa approach by Shen and Zhou [34], which is an unsupervised closed-form method to identify semantic patterns in the latent space  $w$ . It is used to estimate the latent semantic directions in  $w$  that modify particular attributes of the fingerprint while preserving their identity. For instance, by varying the first dimension of  $w$ , we can control the appearance of scribbles in the fingerprint background, while varying the second dimension adds blobs and dry skin artifacts to the fingerprint, as shown in Fig 7. To the best of our knowledge, ours is the first study to introduce such capabilities to fingerprint generation.

#### E. Losses and Training

The proposed scheme is trained in two steps:

**Generator model training.** The first step is to train the ST2-based generator model [20] detailed in Section III-A to synthesize random fingerprints. The generator is trained from

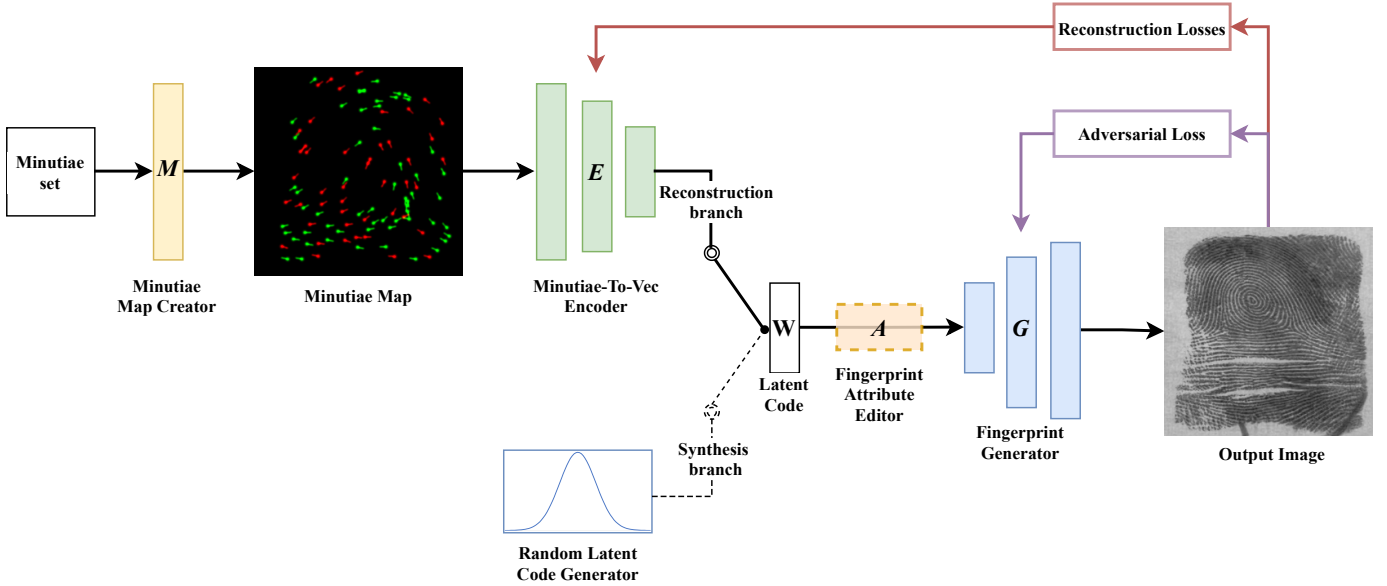


Fig. 2. **The proposed framework.** The proposed fingerprint generator backbone  $\mathbf{G}$  is based on the Stylegan2 architecture. For fingerprint synthesis, the generator is given a normally distributed latent vector  $\mathbf{w}$ . For reconstruction, we first encode the minutiae attributes as a latent vector  $\mathbf{w}$  using the Minutiae-To-Vec encoder network  $\mathbf{E}$ . A fingerprint attribute editor  $\mathbf{A}$  is added before the generator’s input layer, allowing to modify particular attributes of the generated fingerprints, by modifying the latent vector  $\mathbf{w}$ .

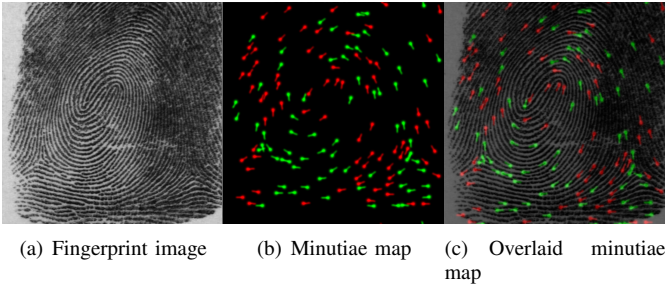


Fig. 3. A fingerprint image from the NIST SD4 dataset and its minutiae map  $\mathbf{M}_x$ . The green and red points are the Termination and Bifurcation minutiae points, respectively. The minutiae orientation is encoded by the angle of the line drawn at each point.

scratch using an uninitialized ST2 model. Training follows the GAN training scheme with an adversarial discriminator loss. The discriminator is alternately fed real and generated fingerprint images, which are used to update the weights of both the generator and discriminator model. We use adaptive discriminator augmentation (ADA) [35] to stabilize training.

**Minutiae-To-Vec Encoder.** The next step is to train the Minutiae-To-Vec Encoder (Section III-C) to embed the minutiae as a latent vector. We freeze the fingerprint generator weights to stabilize the training and use them to generate the reconstructed fingerprint image. The encoder was trained using two losses: the pixelwise  $L_2$  fingerprint reconstruction loss:

$$L_2(\mathbf{x}) = \|\mathbf{x} - \mathbf{G}(\mathbf{E}(\mathbf{M}_x))\|_2, \quad (2)$$

where  $\mathbf{x}$  is the original fingerprint image and  $\mathbf{G}(\mathbf{E}(\mathbf{M}_x))$  is the reconstructed fingerprint image.  $\mathbf{G}$  and  $\mathbf{E}$  are the generator

and encoder models, respectively. A common challenge in reconstruction is to preserve the input’s identity. For that, we apply a pretrained FingerNet CNN [21]

$$L_{id}(\mathbf{x}) = |F_{net}(\mathbf{x}) - F_{net}(\tilde{\mathbf{x}})|, \quad (3)$$

where  $F_{net}(\mathbf{x})$  is the output of the FingerNet CNN consisting of minutiae detection scores, X and Y minutiae probabilities, minutiae orientations, and the segmentation map. The overall reconstruction loss is thus given by

$$L_{recon}(\mathbf{x}) = L_2(\mathbf{x}) + L_{id}(\mathbf{x}). \quad (4)$$

#### IV. EXPERIMENTAL RESULTS

The proposed scheme was experimentally verified by applying it to benchmarks and datasets of rolled fingerprint images used in contemporary state-of-the-art synthesis and reconstruction schemes. The source-codes of most of these schemes, such as Minaee et al. [9], Ross [36], Li and Kot [37] and Feng and Jain [12], are unavailable, and their results are thus cited from other publications.

##### A. Datasets

**NIST SD14.** For fingerprint matching and classification purposes, we used the NIST SD14 dataset [38], which consists of 54,000 rolled fingerprint images obtained from 27,000 unique fingers (with two impressions per finger). This dataset was used to train both the Minutiae-To-Vec encoder and the proposed fingerprint generator.

**NIST SD4.** The NIST SD4 dataset [6] has been commonly employed for testing and building automated fingerprint classification systems. It consists of 4,000 rolled fingerprint images

obtained from 2,000 unique fingers (with two impressions per finger). Fingerprints are classified into five distinct types, each class containing an equal number of prints (400). We utilized this dataset to assess our framework’s performance in both the synthesis and reconstruction tasks.

**SynFing.** The SynFing dataset consists of 100K pairs of synthetic rolled fingerprints created using the proposed fingerprint generator and attribute modifier. Each pair of impressions shares the same synthetic identity but differs in visual attributes, such as scribbles and dry-skin artifacts. We made the SynFing dataset available.

**CaoJain.** We came across only one open source work, the CaoJain dataset, which includes 40,000 synthetic fingerprint images created by Cao and Jain [39]. We generated this dataset to compare and contrast it with the proposed fingerprint synthesis approach.

### B. Implementation Details

The proposed fingerprint generator was applied to the random input  $w \in \mathbb{R}^{512}$ , generating an image  $I \in \mathbb{R}^{512 \times 512}$ . The NIST SD14 dataset was used to train the generator. It was split to 20k, 5k, and 2k fingerprints for the train, validation and test sets, respectively. We preprocessed both the NIST SD14 and NIST SD4 datasets by cropping the fingerprint regions using the FingerNet segmentation CNN [21] and resized them to  $\mathbb{R}^{512 \times 512}$ . The set of minutiae was extracted using Verifinger SDK 11.1 [40]. In the creation of the Minutiae Map  $M_x$  we encoded the bifurcation, termination, and singular points. We drew a line 15 pixels long with an orientation determined by the minute direction for every minute point. The resulting map was smoothed by a Gaussian kernel with  $\sigma = 9$  pixels.

The generator network  $G$  was trained using the Adam optimizer ( $\beta_1, \beta_2 = 0, 0.99$ ) with a batch size of 16. The learning rates of the generator and discriminator were set to 0.0016 and 0.0019, respectively. We used the ADA augmentation policy [35] with a probability of 0.6, and train the model for 480K epochs. The model generates 45 fingerprint images per second on a single NVIDIA GTX 2080 TI GPU. The input to the Minutiae-To-Vec encoder is the minutia map  $M_x \in \mathbb{R}^{512 \times 512 \times 3}$ , and the output is a latent vector  $w \in \mathbb{R}^{512}$ . The encoder was trained using the same dataset (NIST SD14) and splits as the generator. We use the Ranger optimizer with a batch size of 4 and a learning rate of 0.0001 and train the model for 150K epochs.

### C. Fingerprint Synthesis

To estimate the quality of the fingerprint generator, we evaluated the fingerprint realism, distinctiveness, and distribution of minutiae configurations., using the NIST SD4, SynFing, and CaoJain datasets. As NIST SD4 is a dataset of real fingerprints, it estimates the “ideal” fingerprint synthesis method, which is an upper bound of any fingerprint synthesis approach. Samples of each dataset are shown in Fig. 4. Qualitatively, notable

similarities can be seen between the attributes of the NIST SD4 and our SynFing samples. In contrast, the CaoJain images look artificial, and their visual attributes differ significantly from those of the original ones.

#### 1) Fingerprints Validity

For quantitative comparisons, we used the Fréchet Inception Distance (FID) [41], and the NIST Finger Image Quality (NFIQ 2.0) [42] scores. The FID is used to assess the quality of images created by the generative model by comparing the distributions of synthesized and real images. NFIQ 2.0 is an updated open source version of the widely used NFIQ [43], which computes a quality score given a fingerprint image to predict the expected matching performance. The range of NFIQ 2.0 scores is [0, 100], with 0 and 100 being the lowest and highest quality scores, respectively.

Table I presents the FID score for both SynFing and CaoJain, as well as the reported FID score for Minaee et al. [9]. The proposed scheme outperforms the previous schemes by a notable margin. The mean and standard deviation of NFIQ 2.0 values for each of the mentioned datasets are shown in Table II. The average NFIQ 2.0 values for NIST SD4, SynFing, and CaoJain are 44.7, 41.7 and 61.42, respectively. The distribution of our proposed algorithm matches those of the original dataset, while Cao and Jain’s approach [39] exhibits significantly different distributions.

Method	Dataset	FID score
Cao and Jain [39]	NIST SD4	113.82
Minaee et al. [9]	FVC 2006	70.55
Proposed framework	NIST SD4	<b>6.14</b>

TABLE I  
FRÉCHET INCEPTION DISTANCE (FID) FOR DIFFERENT FINGERPRINT SYNTHESIS SCHEMES (LOWER IS BETTER). WE CALCULATED THE FIDS USING 40,000 RANDOM IMAGES GENERATED BY EACH SCHEME. THE SCORE OF MINAAE AT EL. [9] IS CITED AS THERE IS NO OPEN-SOURCE IMPLEMENTATION AVAILABLE.

Dataset	Mean	Std. Dev.
NIST SD4	44.66	17.60
CaoJain	61.42	14.55
SynFing	41.70	16.10

TABLE II  
DISTRIBUTIONS OF NFIQ 2.0 NFIQ 2.0 VALUES ARE [0,100], WHERE 0 AND 100 INDICATE THE LOWEST AND HIGHEST QUALITY VALUES, RESPECTIVELY.

#### 2) Distinctiveness

To evaluate the diversity of our synthetic fingerprints (in terms of identity), we compute pairwise comparison scores for each database using Verifinger SDK 11.1. As long as the impostor score distribution is lower, the generated fingerprints

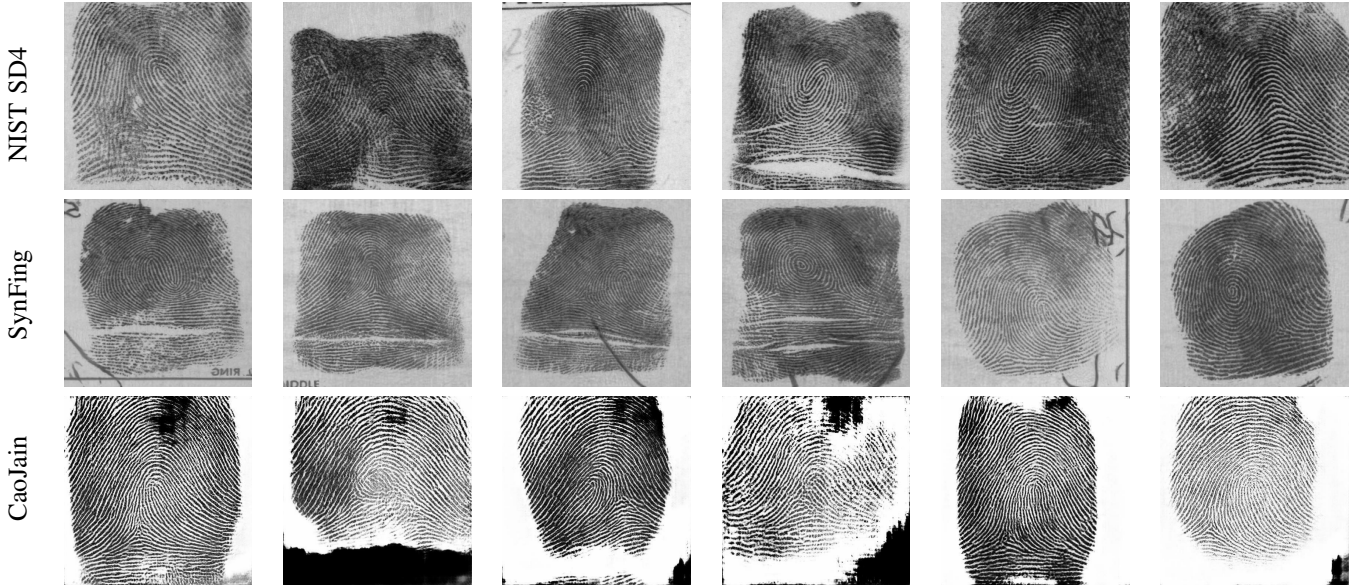


Fig. 4. **Visual Comparison** between NIST SD4 [6], SynFing and CaoJain [39] datasets. The NIST SD4 and SynFing fingerprints are similar, in contrast to the CaoJain samples that look artificial, and their attributes differ significantly from those of NIST SD4.

are more distinct. Figure 5 shows the impostor score distributions. While these score distributions are similar, they vary at the higher range of score values. The maximum impostor comparison scores on NIST SD4, SynFing and CaoJain are 31, 31, and 36, respectively. This indicates the higher diversity of the fingerprints generated by our scheme (in terms of distinctiveness) compared to those generated by the other approaches. Furthermore, this comparison reveals that the number of corrupted fingerprints in CaoJain (identified by Verifinger as 'BadObject') is double that of those detected in SynFing (1.3%).

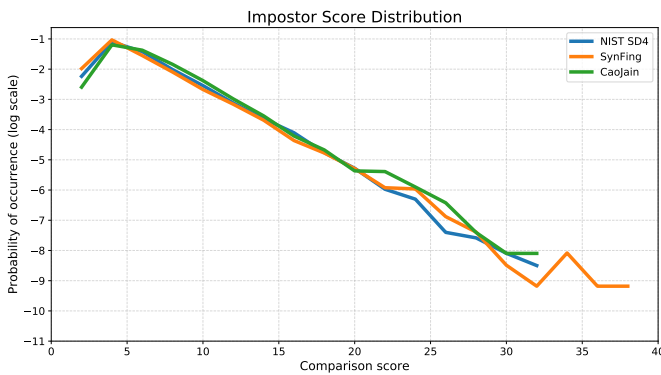


Fig. 5. **Impostor score distributions** for the NIST SD4, SynFing and CaoJain datasets. The comparison scores of the Verifinger SDK 11.1 are [0,6,356]. The higher the score, the more similar are the fingerprint images. The probability of occurrence is shown in a log scale to illustrate the differences for higher values.

### 3) Minutiae Configuration

Fingerprint minutiae are considered the most discriminating features for fingerprint recognition [1]. The spatial distribution of the configurations of the minutiae extracted from

the synthesized fingerprints is an indicator of their realism [16]. Gottschlich and Huckemann [16] showed that the 2D minutiae histogram (2DMH) is effective in differentiating real fingerprint images from synthetic ones. We compared the 2DMH of the SynFing and CaoJain datasets to that of SD4 to evaluate the realism of synthetic fingerprint images. Given a fingerprint image, its set of minutiae is extracted by Verifinger SDK 11.1. Then we build a two-dimensional minutiae histogram by computing the distance  $d$  between the minutiae locations (in pixels) and the angular difference  $\alpha$  (in degrees) of the two minutiae directions for all pairs of minutiae on a template. Both features are binned using identically sized equidistant intervals. Figure 6 presents the average 2DMH for SD4, SynFing, and CaoJain with  $10 \times 10$  bins, where the distances are divided into intervals of 20 pixels, up to a maximum distance of 200 pixels (distance increases from top to bottom). Angular differences are also divided into 10 bins of  $180^\circ$  overall. Each bin of angular differences consists of two intervals of  $18^\circ$  and the differences  $> 180^\circ$  are mirrored.

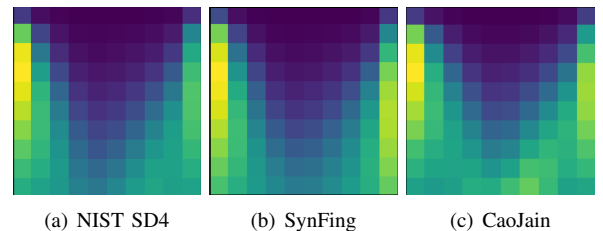


Fig. 6. **Average 2D minutiae histograms**. The vertical axis of each histogram represents the distance  $d$  between minutiae locations, and the horizontal axis shows the angular difference  $\alpha$  between minutiae directions.

Figure 6 shows that the histograms of all the three datasets

are qualitatively similar. Therefore, we computed the Earth Moving Distance (EMD) between the histograms, following Gottschlich and Huckemann [16], to quantitatively compare the different methods. The EMD measured between NIST SD4 and SynFing is 0.42, while that between NIST SD4 and CaoJain is 0.73, indicating that the fingerprint images generated by our approach (SynFing) are more similar to real fingerprint images (NIST SD4) than those of the previous SOTA approach (CaoJain).

#### D. Fingerprints Reconstruction

Reconstructed fingerprints can be used to spoof a system that stores the original fingerprint templates (referred to as a Type-I attack), or other systems where the same finger has been enrolled with a different impression (referred to as a Type-II attack). We evaluated the proposed reconstruction scheme for verification and identification, using the VeriFinger 11.1 fingerprint recognition system and the NIST SD4 dataset.

##### 1) Fingerprint Verification

The verification experiment was carried out using NIST SD4 and Type-I and Type-II attacks. In a Type-I attack, each reconstructed fingerprint is matched against the same impression from which the minutiae template was extracted, while in a Type-II attack, each reconstructed fingerprint is matched against another impression of the same finger, which is more difficult. Based on imposter matching scores, thresholds for different false acceptance rates (FAR) are calculated. In Table III, we report the verification performances of the Type-I and Type-II attacks. As none of the fingerprint reconstruction algorithms are publicly available and as there are no verification results for NIST SD4, we only report the results of the proposed scheme.

FAR	Type-I attack	Type-II attack
1%	99.92%	97.67%
0.1%	99.67%	93.67%
0.01%	99.26%	86.32%
0%	99.23%	85.44%

TABLE III  
VERIFICATION ACCURACY OF THE PROPOSED APPROACH FOR TYPE-I AND TYPE-II ATTACKS AND MULTIPLE FALSE ACCEPT RATES (FAR) USING THE NIST SD4 DATASET.

In the Type-I attack, the matching performance of all four tested FAR are above 99%, implying that in over 99% of cases the proposed framework was able to reconstruct the original fingerprint at a level that *would allow the deception of a commercial fingerprint recognition system*. For the Type-II attack, our results illustrate the ability of the proposed algorithm to reconstruct a fingerprint image while preserving its original attributes.

##### 2) Fingerprint Identification

In the fingerprint identification experiments, minutiae templates of 2,000 file fingerprints from NIST SD4 were used to reconstruct the fingerprints. Each reconstructed fingerprint is compared to 2,000 file fingerprints to obtain 2,000 Type-I attacks, and to 2,000 query fingerprints to obtain 2,000 Type-II attacks. Table IV reports the identification performance for Type-I and Type-II attacks of the proposed approach, as well as the performance of the four other reconstruction schemes by Cao and Jain [13], Feng and Jain [12], Li and Kot [37], and Ross [36].

Method	Type-I attack	Type-II attack
Ross [36]	23.00%	-
Li and Kot [37]	90.80%	24.80%
Feng and Jain [12]	99.70%	65.10%
Cao and Jain [13]	99.05%	71.00%
Proposed framework	<b>99.89%</b>	<b>98.93%</b>

TABLE IV  
THE IDENTIFICATION ACCURACY OF FINGERPRINTS RECONSTRUCTION SCHEMES FOR TYPE-I AND TYPE-II ATTACKS USING THE NIST SD4 DATASET. THE RESULTS OF LI AND KOT [37] ARE CITED [13] AS THEIR IDENTIFICATION RESULTS WERE NOT REPORTED.

The identification accuracy of the proposed reconstruction algorithm is significantly better than that of other reconstruction schemes. For the Type-I attack, the proposed scheme shows almost perfect results. In fact, in 99.9% of cases, the source fingerprint is identified as the best match among all the gallery of 2000 fingerprints. In terms of Type II attack, which is considered more challenging, the proposed algorithm outperforms all other approaches by showing an identification performance of 98.9% compared to 71.0% of Cao and Jain [13], which was the previous SOTA in this task.

##### E. Fingerprint Attribute Modification

Our approach allows the user to generate multiple impressions of the same fingerprint by modifying the attributes of the generated fingerprint, as detailed in Section III-D. To evaluate the performance, we used the proposed SynFing synthetic fingerprint dataset that was split into two subsets. Each subset consists of fingerprints generated by modifying one of the two leading interpretable directions found by investigating the latent space of the proposed generator using the SeFa approach [34]. The first direction affects the presence of scribbles in the fingerprint background, while the second adds blobs and dry-skin artifacts to the generated fingerprint. We refer to these datasets as SynFingP1 and SynFingP2, respectively, which are shown in Fig. 7 and were made publicly available.

Figure 7 shows the varying attributes across multiple impressions, and we quantitatively evaluate the identity preservation across all impressions. Therefore, for each pair of impressions, we compute the matching scores using Verifinger

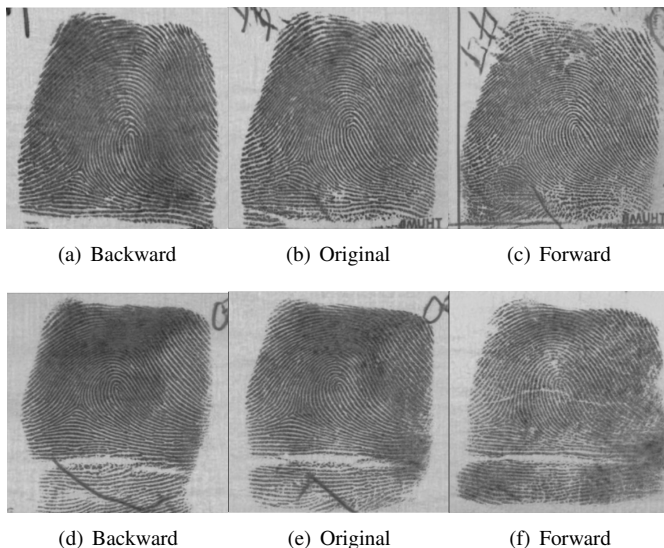


Fig. 7. **The leading directions in the fingerprint embedding space.** **Top row:** SynFingP1, the direction affects the scribbles in the fingerprint background. **Bottom row:** SynFingP2, the direction, modifies the dry-skin artifacts in the generated fingerprint. The middle image is the original reconstruction, while the other images are the results of modifying the embedding forward and backward in the leading direction.

SDK 11.1, and compare them to the pairwise matching scores for random fingerprints from the NIST SD4 dataset. Figure 8 shows the matching score distributions for each dataset. For the NIST SD4 dataset, the impostor and genuine distributions are the same, while those of SynFingP1 and SynFingP2 are only a genuine comparison. The matching scores for SynFingP1 and SynFingP2 are significantly higher than NIST SD4 impostor score and slightly less compared to the genuine score. This implies that the identity of a fingerprint is well-preserved across the generated impressions, yet there is still room for improvement in order to achieve results similar to those of the real fingerprints.

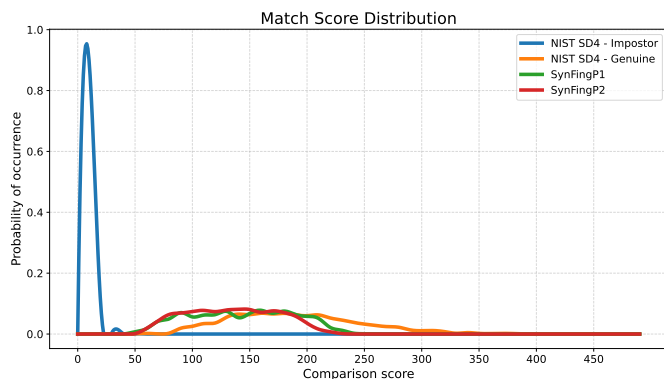


Fig. 8. **Matching score distributions** of the NIST SD4, SynFingP1 and SynFingP2 datasets. The higher the score, the more similar are the fingerprint images. The score distribution for the SD4 dataset relates to impostor comparison, while for SynFingP1 and SynFingP2 it relates to the matching accuracy.

## F. Improving Deep Network Training

One of the main motivations for which we have designed our fingerprint generator is the ability to train a deep learning model using the synthetic dataset to solve a variety of tasks in the field of fingerprints. To evaluate the effectiveness of using our synthetic dataset, we trained three fingerprint matching models, based on the ArcFace architecture [44]. Each model is trained using a different training set, NIST SD14, SynFing, and the combination of the two. The last one was pretrained with the SynFing dataset and then fine-tuned with the NIST SD14 dataset.

The verification accuracy of the three models in the NIST SD4 dataset is detailed in Table V. The model trained with the SynFing dataset is 2% more accurate than the model trained using only the NIST SD14 dataset, while the model trained with both datasets outperforms the two other models by a significant margin. These results demonstrate the effectiveness of using the proposed synthetic fingerprint dataset to augment the limited real fingerprint datasets.

Training Set	Verification Accuracy
NIST SD14	69.20%
SynFing	71.43%
SynFing + NIST SD14	83.72%

TABLE V  
VERIFICATION ACCURACY OF THREE VERIFICATION MODELS TRAINED ON A REAL FINGERPRINT DATASET, A SYNTHETIC FINGERPRINT DATASET, AND THE COMBINATION OF THEM.

## V. CONCLUSIONS

We introduced a new framework in this study for fingerprint synthesis and reconstruction that employs generative adversarial networks. Our approach employs the StyleGan2 architecture as the fingerprint generator for both tasks. We presented a Minutiae-To-Vec encoder that encodes minutia into latent vectors for fingerprint reconstruction and a novel fingerprint synthesis approach that manipulates the attributes of the generated fingerprints while preserving their identity. Our proposed scheme is experimentally shown to outperform state-of-the-art methods for both fingerprint synthesis and reconstruction. This has enhanced the realism of the generated fingerprints, both visually and in terms of spoofing fingerprint-based systems. Additionally, we have shared the SynFing dataset of 100,000 synthetic fingerprint pairs.

## REFERENCES

- [1] D. Maltoni, D. Maio, A. K. Jain, and S. Prabhakar, *Handbook of fingerprint recognition*. Springer Science & Business Media, 2009. 1, 6
- [2] A. K. Jain and A. Kumar, “Biometrics of next generation: An overview,” *Second generation biometrics*, vol. 12, no. 1, pp. 2–3, 2010. 1
- [3] S. Minaee, A. Abdolrashidi, H. Su, M. Bennamoun, and D. Zhang, “Biometrics recognition using deep learning: A survey,” *Artificial Intelligence Review*, 2023. 1



- [4] K. Sundararajan and D. L. Woodard, "Deep learning for biometrics: A survey," *ACM Computing Surveys*, vol. 51, no. 3, pp. 1–34, 2018. 1
- [5] "Nist special database catalog." [Online]. Available: <https://www.nist.gov/srd/shop/special-database-catalog> 1
- [6] C. I. Watson and C. L. Wilson, "Nist special database 4," *Fingerprint Database, National Institute of Standards and Technology*, vol. 17, no. 77, p. 5, 1992. 1, 4, 6
- [7] R. Cappelli, D. Maio, and D. Maltoni, "SFinGe: an approach to synthetic fingerprint generation," in *International Workshop on Biometric Technologies*, 2004, pp. 147–154. 1
- [8] Q. Zhao, A. K. Jain, N. G. Paulter, and M. Taylor, "Fingerprint image synthesis based on statistical feature models," in *2012 IEEE Fifth International Conference on Biometrics: Theory, Applications and Systems (BTAS)*. IEEE, 2012, pp. 23–30. 1
- [9] S. Minaee and A. Abdolrashidi, "Finger-gan: Generating realistic fingerprint images using connectivity imposed gan," *arXiv preprint arXiv:1812.10482*, 2018. 1, 2, 4, 5
- [10] V. Mistry, J. J. Engelsma, and A. K. Jain, "Fingerprint synthesis: Search with 100 million prints," in *IEEE International Joint Conference on Biometrics*. IEEE, 2020, pp. 1–10. 1, 2
- [11] R. Cappelli, D. Maio, A. Lumini, and D. Maltoni, "Fingerprint image reconstruction from standard templates," *IEEE Transactions on Pattern Analysis and Machine Intelligence*, vol. 29, no. 9, pp. 1489–1503, 2007. 1, 2
- [12] J. Feng and A. K. Jain, "Fingerprint reconstruction: from minutiae to phase," *IEEE Transactions on Pattern Analysis and Machine Intelligence*, vol. 33, no. 2, pp. 209–223, 2010. 1, 2, 4, 7
- [13] K. Cao and A. K. Jain, "Learning fingerprint reconstruction: From minutiae to image," *IEEE Transactions on information forensics and security*, vol. 10, no. 1, pp. 104–117, 2014. 1, 2, 7
- [14] J.-H. Moon, J.-H. Park, and G.-Y. Kim, "Restore fingerprints using pix2pix," in *Advances in Computer Science and Ubiquitous Computing*. Springer, 2021, pp. 489–494. 1, 3
- [15] R. Cappelli, D. Maio, and D. Maltoni, "Synthetic fingerprint-database generation," in *Object recognition supported by user interaction for service robots*, vol. 3. IEEE, 2002, pp. 744–747. 1
- [16] C. Gottschlich and S. Huckemann, "Separating the real from the synthetic: minutiae histograms as fingerprints of fingerprints," *IET Biometrics*, vol. 3, no. 4, pp. 291–301, 2014. 1, 2, 6, 7
- [17] I. Goodfellow, "Nips 2016 tutorial: Generative adversarial networks," *arXiv preprint arXiv:1701.00160*, 2016. 1
- [18] M. S. Riazi, S. M. Chavoshian, and F. Koushanfar, "SynFi: Automatic synthetic fingerprint generation," *arXiv preprint arXiv:2002.08900*, 2020. 1
- [19] K. Bahmani, R. Plesh, P. Johnson, S. Schuckers, and T. Swyka, "High fidelity fingerprint generation: Quality, uniqueness, and privacy," in *Proceedings of the IEEE International Conference on Image Processing (ICIP)*, 2021. 1, 2
- [20] T. Karras, S. Laine, M. Aittala, J. Hellsten, J. Lehtinen, and T. Aila, "Analyzing and improving the image quality of stylegan," in *IEEE/CVF Conference on Computer Vision and Pattern Recognition (CVPR)*, 2020, pp. 8110–8119. 2, 3
- [21] Y. Tang, F. Gao, J. Feng, and Y. Liu, "Fingernet: An unified deep network for fingerprint minutiae extraction," in *IEEE International Joint Conference on Biometrics*. IEEE, 2017, pp. 108–116. 2, 4, 5
- [22] R. Cappelli, A. Erol, D. Maio, and D. Maltoni, "Synthetic fingerprint-image generation," in *International Conference on Pattern Recognition (ICPR)*, vol. 3. IEEE, 2000, pp. 471–474. 2
- [23] A. Radford, L. Metz, and S. Chintala, "Unsupervised representation learning with deep convolutional generative adversarial networks," in *International Conference on Learning Representations (ICLR)*, Y. Bengio and Y. LeCun, Eds., 2016. 2
- [24] I. Gulrajani, F. Ahmed, M. Arjovsky, V. Dumoulin, and A. Courville, "Improved training of wasserstein gans," in *Advances in Neural Information Processing Systems (NIPS)*. Red Hook, NY, USA: Curran Associates Inc., 2017, p. 5769–5779. 2
- [25] T. Karras, S. Laine, and T. Aila, "A style-based generator architecture for generative adversarial networks," in *IEEE/CVF Conference on Computer Vision and Pattern Recognition (CVPR)*, 2019, pp. 4401–4410. 2
- [26] K. G. Larkin and P. A. Fletcher, "A coherent framework for fingerprint analysis: are fingerprints holograms?" *Optics Express*, vol. 15, no. 14, pp. 8667–8677, 2007. 2
- [27] H. Kim, X. Cui, M.-G. Kim, and T. H. B. Nguyen, "Reconstruction of fingerprints from minutiae using conditional adversarial networks," in *International Workshop on Digital Watermarking*. Springer, 2018, pp. 353–362. 3
- [28] P. Isola, J.-Y. Zhu, T. Zhou, and A. A. Efros, "Image-to-image translation with conditional adversarial networks," in *IEEE/CVF Conference on Computer Vision and Pattern Recognition (CVPR)*, 2017, pp. 1125–1134. 3
- [29] E. Richardson, Y. Alaluf, O. Patashnik, Y. Nitzan, Y. Azar, S. Shapiro, and D. Cohen-Or, "Encoding in style: a stylegan encoder for image-to-image translation," in *IEEE/CVF Conference on Computer Vision and Pattern Recognition (CVPR)*, 2021, pp. 2287–2296. 3
- [30] X. Luo, X. Zhang, P. Yoo, R. Martin-Brualla, J. Lawrence, and S. M. Seitz, "Time-travel rephotography," *arXiv preprint arXiv:2012.12261*, 2020. 3
- [31] L. Ma, X. Jia, Q. Sun, B. Schiele, T. Tuytelaars, and L. Van Gool, "Pose guided person image generation," *arXiv preprint arXiv:1705.09368*, 2017. 3
- [32] H. Tang, D. Xu, G. Liu, W. Wang, N. Sebe, and Y. Yan, "Cycle in cycle generative adversarial networks for keypoint-guided image generation," in *ACM Computing Surveys*, 2019, pp. 2052–2060. 3
- [33] K. He, X. Zhang, S. Ren, and J. Sun, "Deep residual learning for image recognition," in *IEEE/CVF Conference on Computer Vision and Pattern Recognition (CVPR)*, 2016, pp. 770–778. 3
- [34] Y. Shen and B. Zhou, "Closed-form factorization of latent semantics in gans," in *IEEE/CVF Conference on Computer Vision and Pattern Recognition (CVPR)*, 2021. 3, 7
- [35] T. Karras, M. Aittala, J. Hellsten, S. Laine, J. Lehtinen, and T. Aila, "Training generative adversarial networks with limited data," in *Advances in Neural Information Processing Systems (NIPS)*. Red Hook, NY, USA: Curran Associates Inc., 2020. 4, 5
- [36] A. Ross, J. Shah, and A. K. Jain, "From template to image: Reconstructing fingerprints from minutiae points," *IEEE Transactions on Pattern Analysis and Machine Intelligence*, vol. 29, no. 4, pp. 544–560, 2007. 4, 7
- [37] S. Li and A. C. Kot, "An improved scheme for full fingerprint reconstruction," *IEEE Transactions on Information Forensics and Security*, vol. 7, no. 6, pp. 1906–1912, 2012. 4, 7
- [38] C. I. Watson, "Nist special database 14: Mated fingerprint cards pairs 2 version 2," *tech. rep., Citeseer*, 2001. 4
- [39] K. Cao and A. Jain, "Fingerprint synthesis: Evaluating fingerprint search at scale," in *International Conference on Biometrics (ICB)*. IEEE, 2018, pp. 31–38. 5, 6
- [40] "Verifinger sdk." [Online]. Available: <https://www.neurotechnology.com> 5
- [41] M. Heusel, H. Ramsauer, T. Unterthiner, B. Nessler, and S. Hochreiter, "Gans trained by a two time-scale update rule converge to a local nash equilibrium," *Advances in Neural Information Processing Systems (NIPS)*, vol. 30, 2017. 5
- [42] N. NFIQ, "2.0: Nist fingerprint image quality," Technical report, US National Institute for Standards and Technology, 2016, Tech. Rep. 5
- [43] E. Tabassi, C. Wilson, and C. Watson, "Nist fingerprint image quality," *NIST Res. Rep. NISTIR7151*, vol. 5, 2004. 5
- [44] J. Deng, J. Guo, N. Xue, and S. Zafeiriou, "ArcFace: Additive angular margin loss for deep face recognition," in *IEEE/CVF Conference on Computer Vision and Pattern Recognition (CVPR)*, 2019, pp. 4690–4699. 8